Journal of Molecular Catalysis B: Enzymatic 62 (2010) 32–39

Contents lists available at ScienceDirect

Journal of Molecular Catalysis B: Enzymatic

journal homepage: www.elsevier.com/locate/molcatb

Catalytic properties of a GH10 endo-β-1,4-xylanase from *Streptomyces thermocarboxydus* HY-15 isolated from the gut of *Eisenia fetida*

Do Young Kim[a], Mi Kyoung Han[a], Hyun-Woo Oh[a], Doo-Sang Park[b], Su-Jin Kim[c], Seung-Goo Lee[c], Dong-Ha Shin[d], Kwang-Hee Son[a,*], Kyung Sook Bae[b], Ho-Yong Park[a,*]

[a] *Industrial Bio-materials Research Center, Korea Research Institute of Bioscience and Biotechnology (KRIBB), Daejeon 305-806, Republic of Korea*
[b] *Biological Resources Center, KRIBB, Daejeon 305-806, Republic of Korea*
[c] *Industrial Biotechnology and Bioenergy Research Center, KRIBB, Daejeon 305-806, Republic of Korea*
[d] *Insect Biotech Co. Ltd., Daejeon 305-811, Republic of Korea*

ARTICLE INFO

Article history:
Received 3 June 2009
Received in revised form 26 August 2009
Accepted 28 August 2009
Available online 11 September 2009

Keywords:
Endo-β-1,4-xylanase
Glycoside hydrolase family 10
Streptomyces thermocarboxydus HY-15
p-Nitrophenylcellobioside
PNP-cellobioside

ABSTRACT

A novel GH10 endo-β-1,4-xylanase (XylG) gene from *Streptomyces thermocarboxydus* HY-15, which was isolated from the gut of *Eisenia fetida*, was cloned, over-expressed, and characterized. The XylG gene (1182 bp) encoded a polypeptide of 393 amino acids with a deduced molecular mass of 43,962 Da and a calculated pI of 6.74. The primary structure of XylG was 69% similar to that of *Thermobifida fusca* YX endo-β-1,4-xylanase. It was most active at pH 6.0 and 55 °C. The susceptibilities of xylans to XylG were as follows: oat spelt xylan > birchwood xylan > beechwood xylan. The XylG also showed high activity (474 IU/mg) toward *p*-nitrophenylcellobioside. Moreover, at pH 6.0 and 50 °C, the V_{max} and K_m values of the XylG were 127 IU/mg and 2.51 mg/ml, respectively, for oat spelt xylan and 782 IU/mg and 5.26 mM, respectively, for *p*-nitrophenylcellobioside. A homology model indicated that XylG folded to form a $(\beta/\alpha)_8$-barrel with two catalytic residues of an acid/base (Glu181) and a nucleophile (Glu289). The formation of a disulfide bond between Cys321 and Cys327 were predicted by homology modeling.

1. Introduction

Invertebrates have attracted much attention from bio-industries as sources of a wide variety of gut microorganisms that are expected to have new metabolic pathways or novel genes encoding biocatalysts [1,2]. Accordingly, studies to explore useful biomaterials, such as biopolymers, novel enzymes, and secondary metabolites, from invertebrate-symbiotic microorganisms have been gradually increased. Of the fibrolytic microorganisms present in the digestive tracks of invertebrates, xylanolytic microorganisms are primarily responsible for the degradation of various xylosic materials, which were uptaken as foods by hosts. However, only limited studies evaluating the xylan-degrading exo-symbionts of especially, earthworms have been conducted to date [3].

Recently, many studies have been conducted to evaluate the production of biofuels using various lignocellulosic biomasses; however, biomass recalcitrance still remains as a problem that must be solved to enable the efficient preparation of simple sugars from the bioresources [4]. Accordingly, the development of a suitable enzymatic pretreatment strategy that can facilitate the degradation of lignocellulosic biomasses by selectively eliminating hemicellulose components is necessary to enable the efficient production of glucose or cellobiose from the recalcitrant biomasses. Bioenergy such as bioethanol or biobutanol is produced by microbial transformation of the fermentable saccharides. One of the hemicellulases, endo-β-1,4-xylanases, which give rise to the cleavage of internal β-1,4-xylosidic bonds in the backbone, are the key enzymes responsible for the decomposition of β-1,4-xylan, which is the primary hemicellulose found in plant biomass [5]. These enzymes are currently categorized into five glycoside hydrolase (GH) families (5, 8, 10, 11, and 43) based on their specific fold and catalytic mode. However, most of the known endo-β-1,4-xylanases are incorporated into the following two GH families: GH family 10, which contains endo-β-1,4-xylanases having a molecular mass (>30 kDa) and an acidic pI, and GH family 11, which contains endo-β-1,4-xylanases having a molecular mass (<30 kDa) and a basic pI [6]. Compared to GH11 enzymes, GH10 enzymes are more specific to branched or glucose-derived substrates [7–9] and some of these endo-β-1,4-xylanases are modular enzymes consisting of two or more functional domains in addition to linker regions [10,11].

To date, the three-dimensional structures of more than 10 GH10 endo-β-1,4-xylanases have been clarified by X-ray crystallogra-

* Corresponding authors. Tel.: +82 42 8604650; fax: +82 42 8604659.
E-mail addresses: sonkh@kribb.re.kr (K.-H. Son), hypark@kribb.re.kr (H.-Y. Park).

1381-1177/$ – see front matter © 2009 Published by Elsevier B.V.
doi:10.1016/j.molcatb.2009.08.015

phy analysis [12,13]. All of these enzymes have been found to share significantly similar structures consisting of $(\beta/\alpha)_8$-barrels, additional helices, and loops arranged in a basic triphosphate isomerase-barrel structure that forms an active site cleft [13]. The deep grooves formed by the cleft comprise a series of subsites that are consistent with the endo-fashion of action. The active site amino acids, which play a key role in catalysis and binding to substrates, have also been identified by structural analysis of GH10 endo-β-1,4-xylanase-inhibitor crystals [14] and site-directed mutagenesis [15]. Based on these analyses, it is believed that differences in the substrate specificity of GH10 endo-β-1,4-xylanases are due to the unconserved topology of their substrate-binding clefts [16], although these enzymes show the same gross fold.

In this study, we report the biochemical properties of a novel GH10 endo-β-1,4-xylanase (XylG) from the strain HY-15, a gut bacterium of *Eisenia fetida*, with a strong capacity to hydrolyze *p*-nitrophenylcellobioside (PNP-cellobioside), over-expressed in *Escherichia coli* BL21. In addition, the structural characteristics of XylG predicted by homology modeling are described.

2. Experimental

2.1. Chemicals

β-1,4-D-Xylooligosaccharides of xylobiose to xylotetraose were obtained from Megazyme International Ireland Ltd. (Wicklow, Ireland) and β-1,4-D-cellooligosaccharides of cellobiose to cellotetraose were provided from Seikagaku Biobusiness Co. (Tokyo, Japan). All other chemicals including xylose, PNP-sugar derivatives, and xylans from birchwood, beechwood, and oat spelt were purchased from Sigma Chemical Co. (St. Louis, USA).

2.2. Isolation and identification of a xylan-degrading microorganism

A xylanolytic exo-symbiont, strain HY-15, was isolated from the digestive tract of an earthworm, *E. fetida*, using R2A solid medium (Scharlau Chemie S.A., Barcelona, Spain) that was supplemented with 0.5% (w/v) birchwood xylan, as described in our previous paper [3]. Each liter of R2A solid medium contained 0.75 g peptone, 0.25 g tryptone, 0.5 g yeast extract, 0.5 g dextrose, 0.5 g soluble starch, 0.3 g sodium pyruvate, 0.3 g dipotassium hydrogen phosphate, 0.024 g magnesium sulfate, and 15 g agar. Heterotrophic gut bacteria were cultured on the agar plate for 48 h at 25 °C. Of the xylanolytic microorganisms grown on the medium, strain HY-15 formed a large translucent halo around its colony and was therefore selected for further study. To identify the isolate, sequence analysis of its 16S rRNA gene was conducted as previously described [17]. The 16S rRNA gene sequence of strain HY-15 was aligned with those from strains of the genus *Streptomyces* based on similarities in the primary and secondary RNA structures using the PHYDIT program.

2.3. Cloning of the XylG gene

To amplify a partial fragment of the XylG gene from the genomic DNA, degenerate oligonucleotides were designed based on conserved regions (WDVVNE and VTELDI) in the GH10 endo-β-1,4-xylanases. The upstream primer (GF) was 5′-TGGGACGTCSTCAACGAG-3′ and the downstream primer (GR) was 5′-GATGTCGAGCTCSGTGAC-3′, which produced a 351 bp DNA fragment. The full XylG gene was cloned by repeated DNA walking and nested PCR methods using a DNA Walking *SpeedUp*™ Premix Kit (Seegene Inc., Seoul, Korea).

2.4. Overproduction and purification of XylG

To overproduce XylG, its encoding gene was cloned into the NdeI/HindIII sites of a pET-28a(+) vector (Novagen, Darmstadt, Germany). For this, the full XylG gene with NdeI and HindIII sites in the N-terminus and the C-terminus, respectively, was amplified by PCR using the genomic DNA of *Streptomyces thermocarboxydus* HY-15 as a template. The primer sequences with the NdeI and HindIII sites, respectively, are as follows: the upstream primer (F-GN) was 5′-*CATATG*AGACCCCTTCGTTTCGC-3′ and the downstream primer (R-GH) was 5′-*AAGCTT*TCAGTGCTTAGGGCCCTTCG-3′. The PCR mixture (50 μl) consisted of a PCR buffer, 10 pmol of each primer, 2.5 mM of each dNTP, 20 ng of template DNA, and 2.5 U of FastStart Tag DNA polymerase (Roche Korea Co., Seoul, Korea). A DNA thermal cycler (TaKaRa Korea Biomedical Inc., Seoul, Korea) was used to amplify the XylG gene. The initial template denaturation was conducted for 5 min at 95 °C. Subsequently, the profile, 30 s at 95 °C, 30 s at 53 °C, and 1 min 20 s at 72 °C, was repeated for 30 cycles. The amplified DNA fragment was separated on a 1.0% agarose gel and purified using a HiYield™ Gel/PCR DNA Extraction Kit (Real Biotech Co., Taipei County, Taiwan). The purified PCR products were cloned into a pGEM-T easy vector (Promega, Madison, USA), and the target gene fragment was sequenced. Next, the pGEM-T easy/*xyl*G vectors were digested with NdeI and HindIII, after which the resulting *xyl*G fragments with the corresponding sticky ends were isolated using a HiYield™ Gel/PCR DNA Extraction Kit (Real Biotech Co., Taipei County, Taiwan). To overexpress and purify the XylG, the generated *xyl*G fragments were ligated into a pET-28a(+) vector with the same ends, followed by transformation of the resulting pET-28a(+)/*xyl*G into *E. coli* BL21. Overproduction of the XylG was then conducted by cultivating the recombinant *E. coli* BL21 cells harboring pET-28a(+)/*xyl*G using a 2 l baffle-flask that contained 500 ml of Luria-Bertani broth, in a rotary shaker (180 rpm) for 8 h at 30 °C. The expression of the *xyl*G gene was induced by the addition of 1 mM IPTG after the absorbance of the culture at 600 nm reached approximately 0.4. Following cultivation, the cells were harvested by centrifugation (5000 rpm) and then stored at −20 °C for 1 h. Cell lysis was then conducted using a BugBuster™ Protein Extraction Reagent (Novagen, Darmstadt, Germany), according to the manufacturer's instructions. Following centrifugation (12,000 rpm) for 15 min at 4 °C, the soluble fraction containing the recombinant XylG proteins was collected and then directly used as the crude enzyme source. In this study, enzyme purification was conducted using a HisTrap™ HP (GE Healthcare, Sweden) (5 ml) column and a HiPrep™ 16/10 DEAE FF (Amersham Biosciences, Sweden) column attached to an FPLC system (Amersham Pharmacia Biotech, Sweden). The affinity column chromatography was performed according to the standard protocol provided by the manufacturer, after which the recombinant proteins were eluted using a linear gradient of 0.02–0.5 M imidazole at a flow rate of 1 ml/min. The active fractions were then recovered and desalted with a HiPrep™ 26/10 desalting column (Amersham Biosciences, Sweden) using 20 mM Tris–HCl buffer (pH 7.6) as the mobile phase. For further purification, the resulting enzyme preparation was re-applied to a HiPrep™ 16/10 DEAE FF column that had been pre-equilibrated with 20 mM Tris–HCl buffer (pH 7.6). The recombinant enzyme was then eluted with a gradient of 0–0.5 M NaCl that was applied at a flow rate of 2.0 ml/min. Finally, the active fractions were collected, desalted, and subjected to further analysis.

2.5. Protein analysis

The relative molecular mass of the denatured XylG was determined by SDS-PAGE on a 12% gel. The separated proteins were stained with Coomassie brilliant blue R-250. The protein concentra-

tions were determined using the Bradford reagent (Bio-Rad Korea Ltd., Seoul, Korea).

2.6. Enzyme assays

Endo-β-1,4-xylanase activity was assayed by measuring the amount of reducing sugars produced from birchwood xylan by the 3,5-dinitrosalicylic acid (DNS) method [18] using xylose as a standard. The standard assay mixture (0.5 ml) consisted of 1.0% birchwood xylan and suitably diluted enzyme solution (0.05 ml) in a 50 mM sodium phosphate buffer (pH 6.0) and the enzyme reaction was conducted at 50 °C for 15 min. One international unit (IU) of endo-β-1,4-xylanase activity for xylans was defined as the amount of enzyme required to produce 1 μmol of reducing sugar per min under standard assay conditions. Sugars (5 mM) substituted with *p*-nitrophenol (PNP) were employed to assay other hydrolytic activities of the purified enzyme. The activity assay of XylG toward PNP-sugar derivatives was conducted under the same conditions used in the standard assay of xylanolytic activity. One international unit (IU) of endo-β-1,4-xylanase activity for PNP-sugar derivatives was defined as the amount of enzyme required to produce 1 μmol of PNP per min under standard assay conditions.

2.7. Effects of pH, temperature, and chemicals on the endo-β-1,4-xylanase activity

The optimal pH of the purified XylG was evaluated at a range of 3.5–10.5 using the following buffers (50 mM) at 50 °C for 15 min: sodium citrate (pH 3.5–5.5), sodium phosphate (pH 5.5–7.5), Tris–HCl (pH 7.5–9.0), and glycine–NaOH (pH 9.0–10.5). The effect of temperature on the maximum activity of XylG was determined at 37, 45, 50, 55, 60, 65, and 70 °C under the standard assay conditions. To evaluate the thermostability of XylG, it was pre-incubated at the corresponding temperature for 10, 30, and 60 min in 50 mM sodium phosphate buffer (pH 6.0), after which the enzyme reaction was initiated by adding the substrate to the reaction mixture. The removal of remaining metal ions in the purified enzyme sample was initially conducted by treatment with 20 mM EDTA for 1 h at 4 °C, after which XylG was selectively recovered by a column chromatography using a HiPrep™ 26/10 desalting column (Amersham Phamacia Biotech, Sweden). This enzyme preparation was directly used in the experiments to evaluate the effect of metal ions on the XylG activity. To evaluate the effects on the endo-β-1,4-xylanase activity of metal ions (1 mM) and chemical reagents (5 mM or 0.5%), XylG was pre-incubated at 50 °C for 10 min in 50 mM sodium phosphate buffer (pH 6.0) containing the compound of interest (Table 1) at the indicated concentration. The enzyme reaction was then started by adding the substrate to the reaction mixture. Approximately 2 μg XylG and 1.0% birchwood xylan were used for the reactions.

2.8. Identification of the hydrolysis products

To identify the hydrolysis products, enzymatic degradation of birchwood xylan (10 mg) was conducted using the purified XylG (2 μg) in 0.5 ml of 50 mM sodium phosphate buffer (pH 6.0) for 6 h at 37 °C, during which time the enzyme remained fairly stable. The reaction was then heated to 100 °C for 5 min to stop the enzyme reaction. Similarly, xylooligosaccharides (xylobiose to xylotetraose, each 1 mg) were digested under the same hydrolytic conditions for 3 h. The hydrolysis products were then analyzed by liquid chromatography/tandem mass spectrometry (LC–MS/MS). HPLC analysis was conducted using a Finnigan Surveyor™ Modular HPLC systems (Thermo Electron Co., Waltham, USA) equipped with a Asahipak NH2P-50 2D column (5 μm, 2.0 mm × 150 mm, Shodex) that was operated using the Xcalibur software (version 1.3 SP2, Thermo Electron Co., Waltham, USA). Mobile phase A contained water and 0.05% formic acid, while mobile phase B consisted of acetonitrile and methanol at a ratio of 6:4 in addition to 0.05% formic acid. The gradient elution, which was conducted at a flow rate of 0.25 ml/min was as follows: 0–15 min 85–80% B (linear gradient) and 15–20 min 60% B (isocratic). LC–MS was performed using a Finnigan LCQ Advantage MAX ion trap mass spectrometer (Thermo Electron Co., Waltham, USA) equipped with an electrospray ionization (ESI) source. The mass spectra were obtained in the range m/z 100–1000 in negative ion mode. Data-dependent tandem mass spectrometry (MS/MS) experiments were controlled by the menu-driven software provided with the Xcalibur system. All experiments were performed under automatic gain control conditions.

Table 1
Effects of metal ions (1 mM) and chemical reagents (5 mM) on XylG activity.

Compound	Relative activity (%)
None	100
$HgCl_2$	0
$CaCl_2$	93
$NiSO_4$	103
$CuCl_2$	23
$ZnSO_4$	104
$MgSO_4$	100
$MnCl_2$	142
$SnCl_2$	99
$BaCl_2$	98
$CoCl_2$	127
$FeSO_4$	116
N-Bromosuccinimide	0
Iodoacetamide	41
Sodium azide	57
N-Ethylmaleimide	51
EDTA	41
Dithiothreitol	123
2-Mercaptoethanol	105
Triton X-100 (0.5%)	142
Tween 80 (0.5%)	138

2.9. Homology modeling and structural analysis

The 3D structure of the XylG from *S. thermocarboxydus* HY-15 was generated using the Modeler [19] and Minimization [20] in Discovery Studio 2.0 (Accelrys Inc., San Diego, CA, USA). Comparative modeling was then used to generate the most probable structure of the query protein by alignment with template sequences, simultaneously satisfying spatial restraints, and local molecular geometry. A BLAST search of the PDB database using the XylG sequence exhibited the highest homologies with two endo-β-1,4-xylanases (1E0V and 1V0K) from *Streptomyces lividans*. As a result, these endo-β-1,4-xylanases were utilized as templates for homology modeling after alignment using the Clustal W program. The generated structure was then improved by refinement of the loop conformations by assessing the compatibility of an amino acid sequence with known PDB structures using the Protein Health module in Discovery Studio. All simulation experiments were conducted using an HP XW6200 Workstation with dual Intel Xeon 3.2 GHz processors.

2.10. Nucleotide sequence accession number

The 16S rDNA sequence of the isolate was deposited in GenBank under accession number EU850809. The nucleotide sequence of XylG gene was deposited in GenBank under accession number EU880430.

3. Results

3.1. Identification of a xylanolytic isolate

Phylogenetic analysis of the nucleotide sequence of the strain HY-15 16S rRNA gene revealed that it was closely related to *S. thermocarboxydus* NBRC 16323^T, with a sequence similarity of 99.8%. Based on this result, the isolated strain HY-15 was identified as *S. thermocarboxydus* and deposited in the Korean Collection for Type Cultures under code no. *S. thermocarboxydus* HY-15 KCTC 19532.

3.2. Genetic characterization of XylG gene

The XylG gene isolated in this study contained a 1182 bp open reading frame (ORF) that encodes a protein of 393 amino acids (Fig. 1). A deduced molecular mass (M_r) and a calculated pI of XylG were estimated to be 43,962 Da and 6.74, respectively. It was predicted that the signal peptide cleavage site of premature XylG was between Ala27 and Ala28, which may generate a mature XylG of 366 amino acids with a deduced M_r of 41,354 Da and a calculated pI of 6.46. When the XylG sequence was aligned with other endo-β-1,4-xylanases available in the NCBI database, it was found to possess the molecular features of an endo-β-1,4-xylanase with a sequence similarity similar to that of the GH10 endo-β-1,4-xylanases. However, the sequence similarity levels of XylG with the endo-β-1,4-xylanases in GH family 10 were relatively low. Specifically, the highest sequence similarity was 69%, and this was obtained when XylG was compared to the primary structure of *Thermobifida fusca* YX endo-β-1,4-xylanase (GenBank accession no.: AAZ56824). In addition, XylG was also 69, 59, and 43% identical to *Kineococcus radiotolerans* SRS30216 endo-β-1,4-xylanase (ABS02039), *T. fusca* YX endo-β-1,4-xylanase (ABL73883), and *Acidothermus cellulolyticus* 11B endo-β-1,4-xylanase (ABK52146), respectively. The results of a protein BLAST survey revealed that XylG contained one putative conserved GH10 domain (from Tyr81 to Leu372) that was most similar to the domain structure of GH family 10 (pfam00331). In XylG, the two putative catalytic residues of Glu181 (acid/base catalyst) and Glu289 (catalytic nucleophile), which likely take part in the double-displacement of retaining glycoside hydrolases as indicated by MacLeod et al. [21], were found in highly conserved regions of the active site (Fig. 1).

3.3. Purification and molecular mass of recombinant XylG

In this study, we purified the recombinant XylG to electrophoretic homogeneity by an affinity chromatography and an

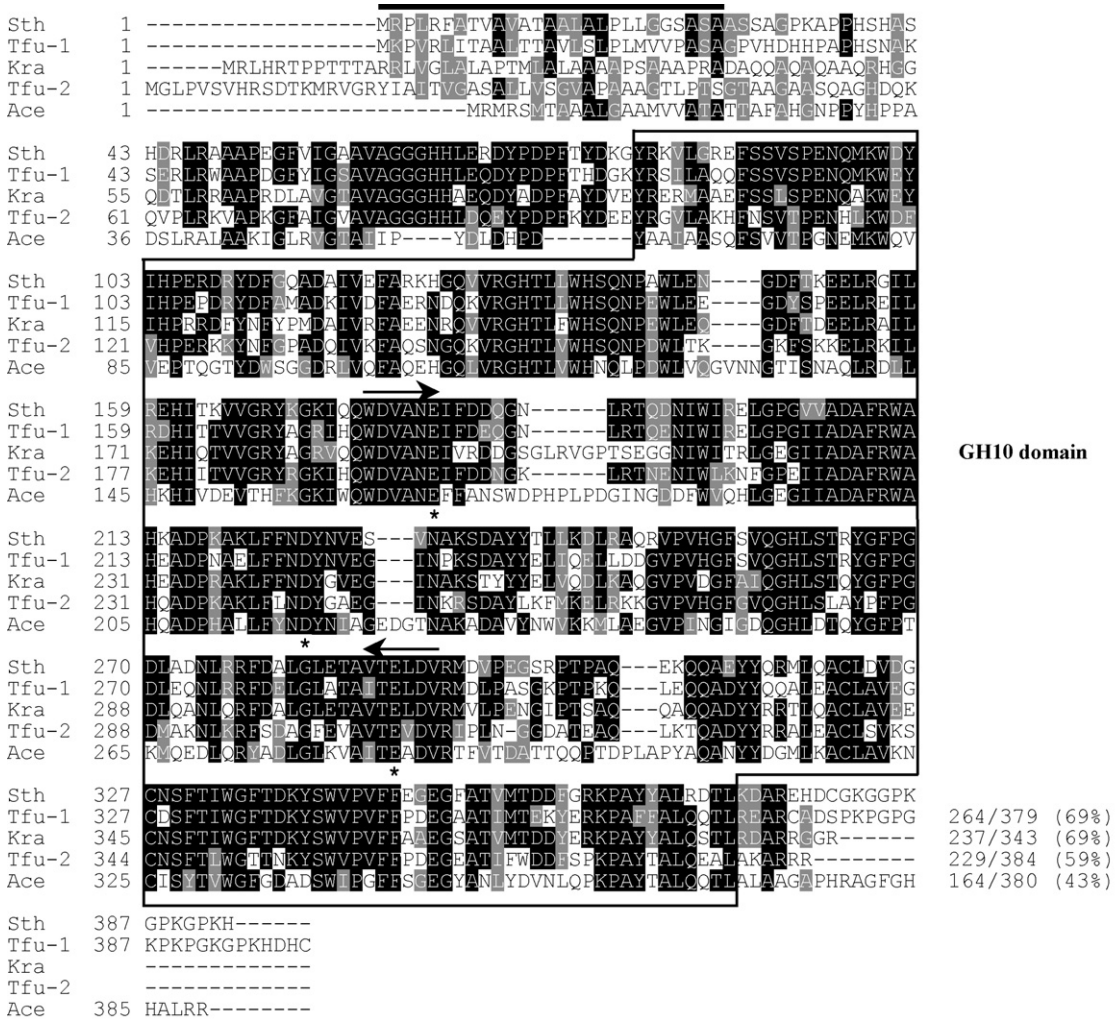

Fig. 1. Alignment of the deduced amino acid sequence of GH10 endo-β-1,4-xylanase from *S. thermocarboxydus* HY-15 with those of other GH10 endo-β-1,4-xylanases. Sequences (GenBank accession number): Sth, *S. thermocarboxydus* HY-15 endo-β-1,4-xylanase (EU880430); Tfu-1, *T. fusca* YX endo-β-1,4-xylanase (AAZ56824); Kra, *K. radiotolerans* SRS30216 endo-β-1,4-xylanase (ABS02039); Tfu-2, *T. fusca* YX endo-β-1,4-xylanase (ABL73883); Ace, *A. cellulolyticus* 11B endo-β-1,4-xylanase (ABK52146). The identical and similar amino acids are shown by black and grey boxes, respectively. The predicted signal peptide is indicated by a black bar. The internal peptide sequences used in the design of degenerate oligonucleotides for PCR reaction are marked by arrows. Highly conserved amino acid residues that play an essential role in the catalytic reaction are indicated by asterisks. GH10 domain is shown by solid-line box.

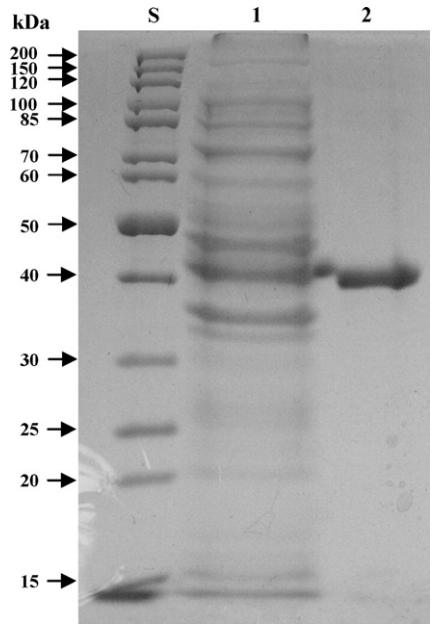

Fig. 2. SDS-PAGE of the purified XylG: lane S, standard marker proteins; lane 1, the soluble cell lysate after IPTG induction; lane 2, purified XylG.

anion exchange chromatography (Fig. 2), as described in Section 2. The recombinant enzyme was released from the HisTrap™ HP column when imidazole was applied at concentrations of 150–200 mM. Additionally, it was also eluted from the DEAE-Sepharose resins when NaCl was applied at concentrations of 250–300 mM. The binding affinity of the recombinant enzyme to the anion exchangers indicates that it is an acidic protein. After the two purification processes, the enzyme was purified 8.5-fold with an overall yield of 56.4%. The M_r of the XylG was estimated to be approximately 40 kDa, as determined by SDS-PAGE (Fig. 2).

3.4. Properties of XylG

The highest catalytic activity of XylG toward birchwood xylan was measured at pH 6.0 (Fig. 3a) and 55 °C (Fig. 3b), and it retained over 85% of its maximum activity at a pH range of 5.0–6.5 (Fig. 3a). However, the hydrolytic ability of XylG for the same substrate was remarkably reduced when the enzyme reaction was conducted at pHs <pH 5.0 or >pH 7.0. Although the XylG retained over 80% of its original activity at temperatures below 45 °C for at least 1 h, its activity was greatly reduced when exposed to temperatures above 55 °C for 10 min (Fig. 3c), indicating that the enzyme reaction should not be performed at 55 °C. Therefore, all subsequent enzyme assays in this study were conducted at 50 °C. At 50 °C, the half-life of XylG was estimated to be approximately 40 min (Fig. 3c).

The XylG completely lost its xylanolytic activity in the presence of Hg^{2+} (1 mM) and *N*-bromosuccinimide (5 mM), indicative of its high sensitivity to these compounds (Table 1). The strong inhibitory effect of XylG exerted by *N*-bromosuccinimide (5 mM) suggests that hydrophobic Trp residues in the active site may play an important role in substrate binding and catalysis. Actually, XylG retained more than 65% of its original catalytic activity when the enzyme assay was conducted in the presence of *N*-bromosuccinimide (5 mM) without pre-incubation with the same inhibitor for 10 min (data not shown). It is likely that the partial inhibition of XylG by *N*-bromosuccinimide occurred because considerable amounts of the enzyme in the reaction mixture were bound to the substrate (birchwood xylan) prior to exposure to the chemical reagent. Apparently, if XylG is bound to the substrate, the important Trp residues in its substrate-binding site will be protected from modification by

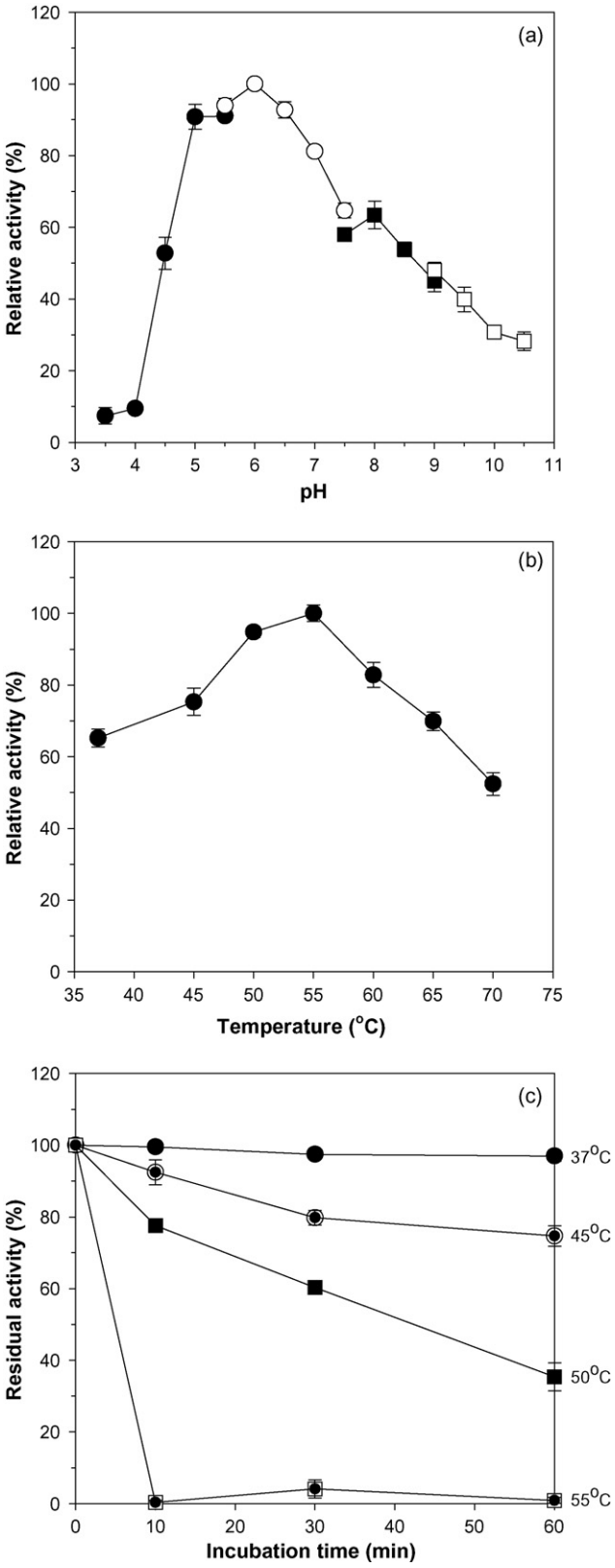

Fig. 3. Effects of pH (a) and temperature (b) on the endo-β-1,4-xylanase activity of XylG and effect of temperature on the stability of XylG (c). The optimal pH of the enzyme was evaluated using the following buffers (50 mM): sodium citrate (●), sodium phosphate (○), Tris–HCl (■), and glycine–NaOH (□).

Table 2
The hydrolysis activity of XylG for different substrates.

Substrate	Specific activity (IU/mg)[a]
Birchwood xylan	70.3 ± 2.3
Beechwood xylan	37.5 ± 1.8
Oat spelt xylan	87.3 ± 3.2
PNP-cellobioside	474 ± 2.5
PNP-glucopyranoside	<0.3
PNP-xylopyranoside	<2.3

[a] Specific activity was obtained from the three repeated experiments.

N-bromosuccinimide. A significant inhibitory effect (>40% of its original activity) on the enzyme activity was also observed when the enzyme was incubated with Cu^{2+} (1 mM), EDTA (5 mM), and the sulfhydryl reagents (each 5 mM), such as iodoacetamide, sodium azide, and *N*-ethylmaleimide. Of the metal ions evaluated, manganese ion (Mn^{2+}) was found to induce an approximately 42% increase in enzyme activity, which is similar to other endo-β-1,4-xylanases [22,23]. In fact, treatment with Ni^{2+} at a concentration of 1 mM had almost no effect on the xylanolytic activity of recombinant enzyme. The catalytic activity of the recombinant XylG increased by approximately 1.4-fold when the enzyme assay was conducted in the presence of nonionic detergents (0.5%) such as Tween 80 and Triton X-100.

3.5. Substrate specificity and kinetic analysis

When compared to xylans (≥90% xylose) from beechwood and birchwood, oat spelt xylan, which consists of xylose (≥70%), glucose (≤15%), and arabinose (≤10%), was most efficiently decomposed by the XylG (Table 2). In this case, the specific activity of the enzyme for oat spelt xylan was determined to be approximately 87.3 IU/mg, which was higher than that of birchwood xylan (70.3 IU/mg) and beechwood xylan (37.5 IU/mg). Based on the results, the susceptibilities of xylosic materials to the XylG were determined to be as follows: oat spelt xylan > birchwood xylan > beechwood xylan. Conversely, glucose-based polysaccharides such as avicel, carboxymethylcellulose (CMC), or soluble starch were not susceptible to XylG. It should be noted that the XylG exhibited high activity (473.5 IU/mg) toward *p*-nitrophenyl (PNP) cellobioside, which is frequently used as a chromogenic substrate to evaluate the exo-cellobiohydrolase activity (Table 2). However, the hydrolysis of PNP-glucopyranoside and PNP-xylopyranoside by the enzyme was negligible.

The Michaelis–Menten kinetic parameters (V_{max} and K_m) for different substrates, which were evaluated from Lineweaver-Burk plots, were determined using xylan (0.2–1.5%) or PNP-cellobioside (2.5–10 mM) as a substrate. Of the polymeric substances evaluated, XylG showed the highest V_{max} value (approximately 127 IU/mg) and a K_m value of approximately 2.51 mg/ml toward oat spelt xylan. Additionally, the V_{max} and K_m values of the recombinant enzyme were 106 IU/mg and 2.11 mg/ml, respectively, for birchwood xylan and of 84 IU/mg and 1.97 mg/ml, respectively, for beechwood xylan. The V_{max} and K_m values of XylG toward PNP-cellobioside were determined to be 782 IU/mg and 5.26 mM, respectively. The catalytic efficiency (V_{max}/K_m) of XylG for oat spelt xylan was higher by approximately 1.01- and 1.19-fold that for birchwood xylan and beechwood xylan, respectively.

3.6. Hydrolysis products of xylosic materials

LC–MS/MS analysis of the hydrolysis products of birchwood xylan that were digested with XylG clearly revealed that the enzyme primarily degraded the polymeric substrate to xylobiose although the small amounts of xylotriose were also produced

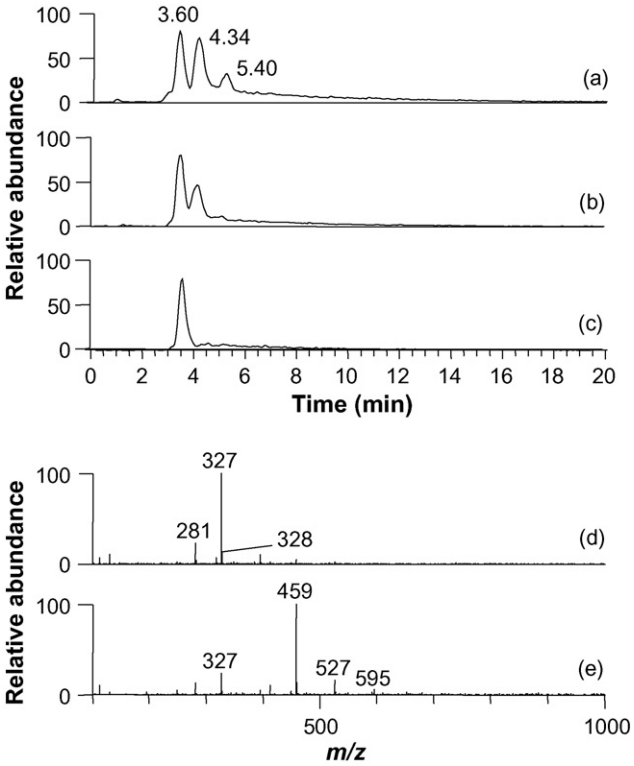

Fig. 4. LC–MS analysis of the hydrolysis products of birchwood xylan: (a) total ion chromatogram of the standards [xylobiose (a peak with a retention time of 3.60 min), xylotriose (a peak with a retention time of 4.34 min), and xylotetraose (a peak with a retention time of 5.40 min)]; (b) total ion chromatogram of the hydrolysis products (3 h reaction); (c) total ion chromatogram of the hydrolysis products (6 h reaction); (d) mass spectrum of a peak with a retention time of 3.60 min; (e) mass spectrum of a peak with a retention time of 4.34 min.

(Fig. 4b), but xylose was not appeared even at the end of hydrolysis reaction (Fig. 4b). Specifically, the molecular ions with a *m*/*z* value of 327 (Fig. 4d) and 459 (Fig. 4e) corresponded to the masses of an adduct of formic acid with xylobiose and xylotriose, respectively. In Fig. 4d, an ion fragment with a *m*/*z* value of 281 also represented the molecular ion of xylobiose. Like birchwood xylan, it was found that xylotriose and xylotetraose were readily degraded by the enzyme, but xylobiose was not further hydrolyzed. It is interesting to note that the XylG could not degrade cellotriose (Fig. 5c) or cellotetraose (Fig. 5d) as well as cellobiose (Fig. 5b) even though it efficiently hydrolyzed PNP-cellobioside, which is often employed as a substrate of cellobiohydrolase. The molecular ions with a *m*/*z* value of 387 (Fig. 5e), 549 (Fig. 5f), and 711 (Fig. 5g) corresponded to the masses of an adduct of formic acid with cellobiose, cellotriose, and cellotetraose, respectively.

3.7. Structural characterization of XylG by homology modeling

The XylG showed the highest sequence identity (69%) with the GH10 endo-β-1,4-xylanase (AAZ56824) of *T. fusca* YX, but no crystal structure was available for this endo-β-1,4-xylanase. Therefore, the homology model of XylG was generated using the crystal structures (1E0V and 1V0K) of *S. lividans* GH10 endo-β-1,4-xylanase as the template, while they showed 40% identity with the XylG of the present study. The homology model of XylG indicated that the mature enzyme may form a $(\beta/\alpha)_8$-barrel with active site loops arranged to form a deep cleft, which is similar to other GH10 endo-β-1,4-xylanases [24]. As expected, two predicted catalytic residues, Glu181 (catalytic acid/base) and Glu289 (catalytic nucleophile), were located within the active site cleft in the model,

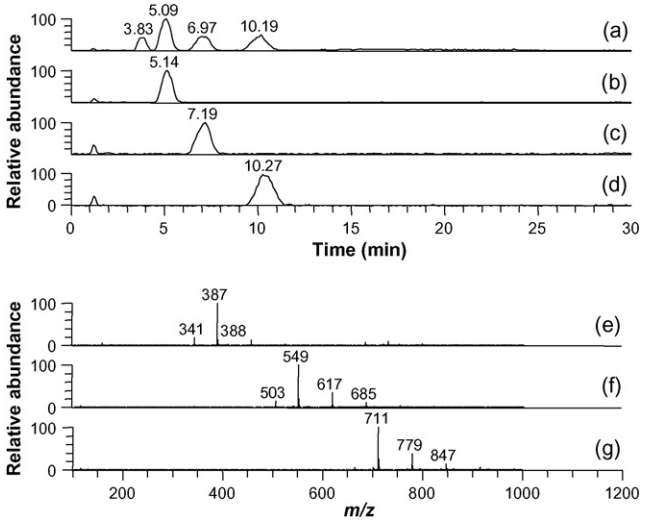

Fig. 5. LC–MS analysis of the hydrolysis products of cellobiose to cellotetraose: (a) total ion chromatogram of the standards [glucose (a peak with a retention time of 3.83 min), cellobiose (a peak with a retention time of 5.09 min), cellotriose (a peak with a retention time of 6.97 min), and cellotetraose (a peak with a retention time of 10.19)]; (b) total ion chromatogram of the hydrolysis products of cellobiose; (c) total ion chromatogram of the hydrolysis products of cellotriose; (d) total ion chromatogram of the hydrolysis products of cellotetraose; (e) mass spectrum of a peak with a retention time of 5.14 min; (f) mass spectrum of a peak with a retention time of 7.19 min; (g) mass spectrum of a peak with a retention time of 10.27 min.

which is in accordance with the catalytic apparatus of a retaining glycoside hydrolase [25]. In addition, a disulfide bridge that takes part in the stabilization of the tertiary structure was predicted between Cys321 and Cys327. Furthermore, the residues of Glu95, Trp136, Ser138, Gln139, Asn180, Glu181, His260, Glu289, Asp291, Arg293, Trp333, Trp341, and Val342 in the active site of XylG were predicted to be within 6 Å around the bound 2-deoxy-2-fluoro-β-D-cellobioside adopted from 1E0V, which is covalently linked to Glu289 in the XylG. Some of these residues are expected to participate in the catalytic reaction or substrate binding of the XylG. However, the presence of the residues within 6 Å distance from the bound oligosaccharide does not necessarily mean that the indicated residues take part in the catalytic reaction or substrate binding because a real substrate (xylan) may have a different orientation in the active site of XylG.

4. Discussion

A number of xylanolytic microorganisms have been isolated and identified from various ecosystems and as a result, many endo-β-1,4-xylanases with distinct properties have been characterized to the molecular level [26]. However, relatively few studies regarding invertebrate-symbiotic xylanolytic bacteria and their related enzymes have been conducted to date, despite that invertebrates such as insects and earthworms may contain a variety of bacteria that express novel fibrolytic enzymes in their guts [2].

In this study, XylG showed the sequence identities (≤69%) when compared to the primary sequences of other similar GH10 enzymes shown in Fig. 1. These low sequence identities indicate that XylG is a new GH10 endo-β-1,4-xylanase with a distinct primary structure that differentiates it from previously identified GH10 endo-β-1,4-xylanases. The molecular architecture of XylG that consists of one functional GH10 domain (from Tyr81 to Leu372) was similar to that of GH10 enzymes from *Clavibacter michiganensis* (YP 001222417), *Cellulosimicrobium* sp. HY-12 (EU179736), and *A. cellulolyticus* 11B (YP 872132). Conversely, the GH10 endo-β-1,4-xylanases of *Cellulomonas fimi* (M15824), *Thermobifida alba* (CAB02654), and *S. lividans* (P26514) are modular enzymes that contain a carbohydrate-binding motif 2, cellulose-binding domain II, and RICIN domain, respectively, as well as a GH10 domain.

No report regarding thermophilic or cold-adapted endo-β-1,4-xylanases from intestinal microorganisms has been published to date. XylG was a typical mesophilic enzyme with the half-life of 40 min at 50 °C and its optimal pH (6.0) of XylG was similar to that of endo-β-1,4-xylanases from insect-symbiotic microorganisms [11,22,23] and a soil isolate, *Streptomyces cyaneus* SN32 [27]. However, many endo-β-1,4-xylanases from free-living microorganisms exhibited the maximum catalytic activity at an acidic pH range of 4.0–5.5 or an alkaline pH range of 8.0–10.0 [6,26]. Similar to some of endo-β-1,4-xylanases [28–31], XylG was also found to be greatly inactivated by Hg^{2+}. However, suppression of *Bacillus halodurans* S7 GH10 endo-β-1,4-xylanase by Hg^{2+} was relatively insignificant [32]. It is considered that the inhibition of XylG by the heavy metal ion may be attributed to its interaction with the sulfhydryl group of Cys380, which may participate in catalysis. This presumption is in good agreement with the fact that XylG was also sensitive to sulfhydryl reagents such as sodium azide, iodoacetamide, and *N*-ethylmaleimide (Table 1) and three Cys residues (Cys321, Cys327, and Cys380) are present in premature XylG (Fig. 1). Accordingly, the formation of a disulfide bond between Cys321 and Cys327 residues in the active site was predicted by the homology model of XylG. In a previous paper, Roberge et al. [33] reported that three Trp residues (W85, W266, and W274) in the active site of GH10 endo-β-1,4-xylanase A from *S. lividans* were critically involved in stacking interactions with xylan and the catalytic function of the enzyme. In addition, the aromatic amino acids are highly conserved in other GH10 enzymes [33] and correspond to the residues of W136, W333, and W341 in premature XylG (Fig. 1). Based on these facts, the complete inactivation of XylG by *N*-bromosuccinimide may be closely related to the modification of the corresponding Trp residues in the active site. *N*-Bromosuccinimide has also been found to have significant negative effects on the hydrolytic activity of endo-β-1,4-xylanases from *Paenibacillus* sp. HY-8 [22] and *Arthrobacter* sp. MTCC 5214 [31]. Nonionic detergents such as Triton X-100 and Tween 80 generally negatively influence the hydrophobic interaction between an enzyme and a substrate. Indeed, the results of a study we recently conducted showed that the wild type endo-β-1,4-xylanase from *Cellulosimicrobium* sp. HY-13 KCTC 11302BP was partially inhibited by these detergents [3]. However, the nonionic detergents (0.5%) in this study induced an increase of the catalytic activity of His-tagged XylG by approximately 1.4-fold. To the best of our knowledge, this is the first report that describes a stimulatory effect of the nonionic detergents on the activity of His-tagged endo-β-1,4-xylanase.

XylG is an endo-β-1,4-xylanase having broad substrate specificity that is able to efficiently decompose heteropolymeric oat spelt xylan consisting of various constituents. However, the GH10 enzymes from *Cellulosimicrobium acetobutylicum* ATCC 824 [28] and *B. halodurans* S7 [32] have been reported to be most efficiently degrade birchwood xylan. The XylG did not show any detectable hydrolysis activities toward cellooligosaccharides of cellobiose to cellotetraose, carboxymethylcellulose (CMC), avicel, or soluble starch, even though many microbial endo-β-1,4-xylanases have been reported to have considerable endo-cellulolytic activities [34]. Taken together, these findings indicate that the recombinant enzyme is not a multi-functional endo-type hydrolase, but a true endo-β-1,4-xylanase that only cleaves the β-1,4-xylosidic linkages in different xylosic compounds. The strong ability of the XylG to hydrolyze the agluconic linkage of PNP-cellobioside is unique because the known endo-β-1,4-xylanases that have been evaluated to date have exhibited relatively weak (<10.0 IU/mg) or no cleavage activity toward the same substrate [3,23,28,29]. The

present results clearly demonstrate that the recombinant enzyme is able to cleave the agluconic bond between *p*-nitrophenol and glucose moieties, but that they have no effect on the gluconic bond. In a previous study, Haga et al. [8] demonstrated that a GH10 endo-β-1,4-xylanase from *Cellvibrio gilvus* had substrate specificities similar to those of XylG toward PNP-cellobioside and cellooligosaccharides. However, the cleavage activity of *C. gilvus* enzyme toward PNP-cellobioside was approximately 65-fold lower than that of XylG toward the same substrate. The above results indicate that the XylG is a peculiar cellulase-free endo-β-1,4-xylanase that has a strong ability to cleave the agluconic bond of PNP-cellobioside in addition to the internal β-1,4-xylosidic bonds on the xylan backbone. The strong PNP-cellobioside cleavage activity will be useful to differentiate a cellulase-free xylanase with high PNP-cellobioside-degrading activity from other structurally similar GH10 enzymes.

5. Conclusions

The XylG from *S. thermocarboxydus* HY-15 is a novel GH10 endo-β-1,4-xylanase that is distinguished from other enzymes in GH family 10 by its primary structure, susceptibility to chemical reagents, and substrate specificities. Although the XylG showed a strong capacity to degrade PNP-cellobioside when compared to other known endo-β-1,4-xylanases, the inability of the enzyme to hydrolyze glucose-derived substrates such as CMC, avicel, cellotriose, and cellotetraose strongly indicates that it is a true cellulase-free enzyme. Compared to some bacterial and fungal endo-β-1,4-xylanases exhibiting high hydrolytic activity toward birchwood xylan (≥90% xylose) [28,32,35], XylG is more active toward oat spelt xylan (≥70% xylose) composed of various constituents. Because of its high substrate affinity to heteropolymeric xylosic materials, the XylG will be useful in the development of a strategy, which enables the efficient preparation of fermentable sugars from a wide range of raw hemicellulosic plant biomass, especially crops such as corn, which are used as sources for the production of bioethanol. Furthermore, when compared to commercial fungal endo-β-1,4-xylanases, which generally have an optimum pH in ranges of 4.0–5.5 [6], XylG has an optimum pH of 6.0. Considering that cellulolytic and hemicellulolytic enzymes in the rumen of herbivorous animals exhibit the highest catalytic activity between pH 6.0 and 6.5 [36], XylG is a potential candidate for the development of an effective feed additive that can aid in the digestion of hemicellulosic foods by herbivorous animals.

Acknowledgements

This work was supported by a grant from KRIBB Research Initiative Program (KGS2330911) and the 21C Frontier Microbial Genomics and Applications Center Program (MGM0900837) of the Korean Ministry of Education, Science and Technology.

References

[1] Y. Brennan, W.N. Callen, L. Christoffersen, P. Dupree, F. Goubet, S. Healey, M. Hernández, M. Keller, K. Li, N. Palackal, A. Sittenfeld, G. Tamayo, S. Wells, G.P. Hazlewood, E.J. Mathur, J.M. Short, D.E. Robertson, B.A. Steer, Appl. Environ. Microbiol. 70 (2004) 3609–3617.
[2] A. Brune, Trends Biotechnol. 16 (1998) 16–21.
[3] D.Y. Kim, M.K. Han, J.S. Lee, H.-W. Oh, D.-S. Park, D.-H. Shin, K.S. Bae, K.-H. Son, H.-Y. Park, Proc. Biochem. 44 (2009) 1055–1059.
[4] M.E. Himmel, S.Y. Ding, D.K. Johnson, W.S. Adney, M.R. Nimlos, J.W. Brady, T.D. Foust, Science 315 (2007) 804–807.
[5] D. Shallom, Y. Shoham, Curr. Opin. Microbiol. 6 (2003) 219–228.
[6] M.L.T.M. Polizeli, A.C.S. Rizzatti, R. Monti, H.F. Terenzi, J.A. Jorge, D.S. Amorim, Appl. Microbiol. Biotechnol. 67 (2005) 577–591.
[7] V. Ducros, S.J. Charnock, U. Derewenda, Z.S. Derewenda, Z. Dauter, C. Dupont, F. Shareck, R. Morosoli, D. Kluepfel, G.J. Davies, J. Biol. Chem. 275 (2000) 23020–23026.
[8] K. Haga, M. Kitaoka, Y. Kashiwagi, T. Sasaki, H. Taniguchi, Agric. Biol. Chem. 55 (1991) 1959–1967.
[9] G. Pell, E.J. Taylor, T.M. Gloster, J.P. Turkenburg, C.M. Fontes, L.M. Ferreira, T. Nagy, S.J. Clark, G.J. Davies, H.J. Gilbert, J. Biol. Chem. 279 (2004) 9597–9605.
[10] G.W. Black, G.P. Hazlewood, S.J. Millward-Sadler, J.I. Laurie, H.J. Gilbert, Biochem. J. 307 (1995) 191–195.
[11] A.E. Cazemier, J.C. Verdoes, A.J.J. Van Ooyen, H.J.M. Op Den Camp, Appl. Environ. Microbiol. 65 (1999) 4099–4107.
[12] Z. Fujimoto, A. Kuno, S. Kaneko, S. Yoshida, H. Kobayashi, I. Kusakabe, H. Mizuno, J. Mol. Biol. 300 (2000) 575–585.
[13] A. Schmidt, A. Schlacher, W. Steiner, H. Schwab, C. Kratky, Protein Sci. 7 (1998) 2081–2088.
[14] V. Notenboom, C. Birsan, R.A.J. Warren, S.G. Withers, D.R. Rose, Biochemistry 37 (1998) 4751–4758.
[15] S.J. Charnock, J.H. Lakey, R. Virden, N. Hughes, M.L. Sinnott, G.P. Hazlewood, R. Pickersgill, H.J. Gilbert, J. Biol. Chem. 272 (1997) 2942–2951.
[16] S.J. Charnock, T.D. Spurway, H. Xie, M.H. Beylott, R. Virden, R.A.J. Warren, G.P. Hazlewood, H.J. Gilbert, J. Biol. Chem. 273 (1999) 32187–32199.
[17] H.J. Kim, D.Y. Kim, J.S. Nam, K.S. Bae, Y.H. Rhee, Antonie van Leeuwenhoek 83 (2003) 183–189.
[18] G.L. Miller, Anal. Chem. 31 (1959) 426–428.
[19] A. Sali, T.L. Blundell, J. Mol. Biol. 234 (1993) 779–815.
[20] F.A. Momany, R.J. Rone, Comp. Chem. 13 (1992) 888–900.
[21] A.M. MacLeod, T. Lindhorst, S.G. Withers, R.A.J. Warren, Biochemistry 33 (1994) 6371–6376.
[22] S.Y. Heo, J. Kwak, H.-W. Oh, D.-S. Park, K.S. Bae, D.H. Shin, H.-Y. Park, J. Microbiol. Biotechnol. 16 (2006) 1753–1759.
[23] H.-W. Oh, S.Y. Heo, D.Y. Kim, D.-S. Park, K.S. Bae, H.-Y. Park, Antonie van Leewenhoek 93 (2008) 437–442.
[24] T. Collins, C. Gerday, G. Feller, FEMS Microbiol. Rev. 29 (2005) 3–23.
[25] P. Biely, M. Vršanská, M. Tenkanen, D. Kluepfel, J. Biotechnol. 57 (1997) 151–166.
[26] N. Kulkarni, A. Shendye, M. Rao, FEMS Microbiol. Rev. 23 (1999) 411–456.
[27] S. Ninawe, M. Kapoor, R.C. Kuhad, Bioresour. Technol. 99 (2008) 1252–1258.
[28] M.K. Ali, F.B. Rudolph, G.N. Bennett, J. Ind. Microbiol. Biotechnol. 32 (2005) 12–18.
[29] H.L. Cheng, P.M. Wang, Y.C. Chen, S.S. Yang, Y.C. Chen, Bioresour. Technol. 99 (2008) 227–231.
[30] J.X. Heck, L.H. De Barros Soares, P.F. Hertz, M.A.Z. Ayub, Biochem. Eng. J. 32 (2006) 179–184.
[31] R.D.S. Khandeparkar, N.B. Bhosle, Enz. Microb. Technol. 39 (2006) 732–742.
[32] G. Mamo, R. Hatti-Kaul, B. Mattiasson, Enz. Microb. Technol. 39 (2006) 1492–1498.
[33] M. Roberge, F. Shareck, R. Morosoli, D. Kluepfel, C. Dupont, Protein Eng. 12 (1999) 251–257.
[34] S. Subramaniyan, P. Prema, FEMS Microbiol. Lett. 183 (2000) 1–7.
[35] I. Romanowska, J. Polak, S. Bielecki, Appl. Microbiol. Biotechnol. 69 (2006) 665–671.
[36] D.P. Morgavi, K.A. Beauchemin, V.L. Nsereko, L.M. Rode, A.D. Iwaasa, W.Z. Yang, T.A. McAllister, Y. Wang, J. Dairy Sci. 83 (2000) 1310–1321.